

Supporting Online Material for:

Supramolecular Packing Controls H₂ Photocatalysis in Chromophore Amphiphile

Hydrogels

Adam S. Weingarten^{1,2}, Roman V. Kazantsev^{1,2}, Liam C. Palmer^{1,3}, Daniel J. Fairfield⁴, Andrew
R. Koltonow⁴, and Samuel I. Stupp^{1,2,3,4,5,6 *}

¹Department of Chemistry, Northwestern University, Evanston, Illinois 60208, USA.

²Argonne-Northwestern Solar Energy Research (ANSER) Center, Northwestern University,
Evanston, Illinois 60208, USA.

³Simpson Querrey Institute for BioNanotechnology, Northwestern University, Chicago, Illinois
60611, USA

⁴Department of Materials Science and Engineering, Evanston, Illinois 60208, USA.

⁵Department of Medicine, Northwestern University, Chicago, Illinois 60611, USA

⁶Department of Biomedical Engineering, Northwestern University, Evanston, Illinois 60208,
USA.

*To whom correspondence should be addressed.

E-mail: s-stupp@northwestern.edu

Table of Contents

Materials

Methods

Synthesis

Recycling GPC Traces for CA Purification

SAXS Pattern for CA Linker Series Without Added Salt

Model Fits for CA Linker Series SAXS Data

Solution State WAXS Data and Tables

WAXS for CAs with NaCl

Nanostructure Thickness versus Methylene Number

AFM Images of CA Linker Series

GIXS Diffraction Peak Tabulation

DMSO and Water Absorbance Data for CA Linker Series

Chemical Structure of **P2N2** Nickel Catalyst

Absorbance of CA Gels in Photocatalysis Media

SEM Images of CA Linker Series PDDA Gels

Images of CA Linker Series PDDA Gels in Aqueous Ascorbate Solutions

H₂ Photosensitization Data from **L3**

Emission Data for CA Linker Series

Materials

Water used for assembly experiments was passed through a Barnstead Nanopure (D3750 hollow fiber filter, 0.2 μm pore size) and UV-irradiated to achieve 18.2 M Ω -cm purity before use. Perylene monoanhydride¹ and **P2N2** nickel catalyst² were synthesized according to reported methods. ω -Aminohexanoic acid was purchased from TCI. Anhydrous potassium carbonate was purchased from EMD. Concentrated HCl (30% in water) was purchased from Macron Fine Chemicals and diluted to 2M before use. Absolute ethanol, sodium hydroxide, and chloroform were also purchased from Macron Fine Chemicals. NaCl, PDDA (medium molecular weight, 20 wt% in water), β -alanine 99%, 4-aminobutyric acid, and 10-bromodecanoic acid 95% were purchased from Sigma–Aldrich. $\text{Zn}(\text{OAc})_2 \cdot 2\text{H}_2\text{O}$ was purchased from Strem Chemicals. *N,N'*-dimethylformamide (DMF) was purchased from BDH and dried using a Vacuum Atmospheres Co. solvent purifier. Concentrated sulfuric acid and dimethylsulfoxide (DMSO) were also purchased from BDH. Ascorbic acid, 98% oxalyl chloride, ammonia 50%, glycine 99%, 5-aminovaleric acid, and 8-aminooctanoic acid 95% were purchased from Alfa Aesar. NMR spectra were acquired using a 400 MHz Agilent DD MR-400 or a Bruker AVANCE III (500 MHz, direct cryoprobe). High-resolution mass spectrometry was acquired using an Agilent 6210 LC-TOF (ESI, APCI, APPI).

The lamp utilized has a roughly Gaussian emission around 600 nm, far to the red where these PMIs primarily absorb. From the absorbance data, the shorter linkers absorb more to the blue than the longer linkers, biasing hydrogen photosensitization studies against the short-linker PMI gels. To address this, we investigated a different lamp with an emission maximum at 550 nm, shifting the spectrum roughly 50 nm. However, we observed only 200 TONs for the L5 derivative and almost no hydrogen from the L1.

Methods

Cryogenic transmission electron microscopy (Cryo-TEM)

Cryo-TEM imaging was performed on a JEOL 1230 microscope, operating at 80 kV. A 5.5 μL droplet was placed on a lacey carbon film supported on a TEM copper grid. The grid was held by tweezers mounted on a Vitrobot Mark IV equipped with a controlled humidity and temperature environment. The specimen was blotted and plunged into a liquid ethane reservoir cooled by liquid nitrogen. The vitrified samples were transferred to a Gatan 626 cryo-holder through a cryo-transfer stage cooled by liquid nitrogen. During observation of the vitrified samples, the cryo-holder temperature was maintained below -180°C . The images were recorded with a CCD camera.

Small angle X-ray scattering (SAXS)

SAXS measurements were performed using beam line 5ID-D, in the DuPont-Northwestern-Dow Collaborative Access team (DND-CAT) Synchrotron Research Center at the Advanced Photon Source, Argonne National Laboratory. X-ray energy of 15 keV corresponding to a wavelength of 0.83 \AA^{-1} was selected using a double-crystal monochromator. The data were collected using a CCD detector (MAR) positioned 245 cm behind the sample. The scattering intensity was recorded in the interval $0.002 < q < 0.12 \text{ \AA}^{-1}$. The wave vector defined as

$$q = (4\pi / \lambda) \sin(\theta/2)$$

where θ is the scattering angle. Samples were placed in 1.5 mm quartz capillaries. The exposure times were between 2 and 4 seconds.

Prior to experimentation, aqueous solutions of PMI were diluted with DMSO to break up assemblies and then freeze-dried to remove solvent. Samples are then dissolved to prepare 50 μL of 11.5 mM PMI solutions to which are added 10 μL of water (for account for dilution) or 300 mM NaCl (for screening studies).

Atomic force microscopy (AFM)

AFM measurements were performed using a Parks Systems XE-100 under tapping mode. Samples (4 μL , 115 μM) were drop cast and air-dried on a freshly cleaved mica substrate that had been treated with 300 mM MgCl_2 to render the mica surface cationic and promote nanostructure adhesion.

Scanning electron microscopy (SEM)

SEM was performed on a Hitachi S-4800 II SEM. Critical-point drying was used to preserve the structure of the gel samples during SEM analysis. After gel preparation, the water was exchanged with ethanol using a gradient of ethanol/water mixtures. The gels were transferred to a stainless steel cage with wire mesh and soaked in 25% ethanol/water solution for 10 minutes. The cage was transferred to a 50% ethanol solution and so repeated for 60%, 70%, 80%, 90%, 95%, and 100% ethanol solutions. The ethanol-exchanged samples were then critically point dried using a Tousimis Samdri 795 with supercritical CO₂ and a 10 minute purge timer. Samples were coated with 20 nm of osmium metal using a Filgen Osmium Plasma Coater OPC60A.

Wide Angle X-ray Scattering (WAXS)

WAXS was collected at Argonne National Lab's Advanced Photon Source, in BioCARS sector 14-BM-C. Samples were prepared by mixing 20 μ L of CA (11.5 mM) with 4 μ L water, 5 wt% PDDA, or 300 mM NaCl. Solutions or hydrated gels (4 μ L) were placed on MiTeGen MicroMounts (M1-L18SP-400) and irradiated with 0.979 \AA X-ray light (12.669 KeV) for 20 seconds. Samples were replaced after two exposures to avoid measuring dried samples. Data were collected using an ADSC Quantum 315 detector placed 400 mm from the sample. Samples were calibrated to a CeO₂ standard. The intensity of the 2D plots was integrated to produce 1D plots presented in figures.

Grazing Incidence X-ray Scattering (GIXS)

GIXS was collected at Argonne National Lab's Advanced Photon Source, in sector 8-ID-E. The beam energy was 7.35 KeV, with an incident angle of 0.3°. Samples were prepared by placing a 100 μ L droplet of 11.5 mM CA solution onto a glass slide and allowing the droplet to dry in air.

The nanostructure thicknesses were obtained by converting the observed primary scattering peak (in \AA^{-1}) to the real-space distance (\AA) as shown below. The distance between the core PMI and the exterior surface carboxylate was estimated by subtracting the length of the aromatic PMI core (10.5 \AA , from the H on the 9-position to the imide N) from the calculated

nanostructure thickness (obtained from conversion of the primary scattering peak in the GIXS z-axis to a real-space distance) and dividing the difference by two (as the proposed anti-parallel packing should place the alkyl linker above and below the nanostructures' PMI core) according to the following equation:

$$X = \frac{d - 10.5}{2}$$

Where X is the distance between the PMI core and the exterior carboxylate surface and d is the real-space distance calculated from the primary GIXS scattering peak in the Z-axis. For a diagram, see Figure S7.

Calculations

Conversion of inverse space (\AA^{-1}) to real-space distances (\AA)

The peaks obtained in X-ray experiments are converted from inverse space (q) to real space (d) through the following relation:

$$d = \frac{2\pi}{q}$$

2D Unit Cell

The unit cell parameters of CA crystals were determined using the following geometric analysis. Specifically, the three observed peaks correspond to vectors of an inverse-space triangle of dimensions a^* (or 1 0 vector), b^* (or 0 1 vector), and $(a+b)^*$ (or 1 1 vector), the order in which peaks are labelled in moving from lower to higher q values. The real-space dimensions of the 2D oblique lattice a (1 0), b (0 1), and θ are calculated as follows:

$$\theta^* = \cos^{-1} \left(\frac{(a^*)^2(b^*)^2 - (a^* + b^*)^2}{2a^*b^*} \right)$$

$$\theta = 180 - \theta^*$$

$$a = \frac{2\pi}{a^* \sin \theta}$$

$$b = \frac{2\pi}{b^* \sin \theta}$$

Pi-stacking distance

Pi-stacking distances are calculated according to the following:

$$\pi \text{ stacking} = b \sin \theta$$

Where b is the real-space, short-edge of the calculated 2D unit cell or $(0\ 1)$ vector and θ is the angle calculated above.

Ultraviolet – Visible Absorbance Spectroscopy

Absorbance spectroscopy on aqueous CA solutions (9.57 mM) was performed in a 0.05 mm path length, closed demountable quartz spectrophotometer cell (Starna Cells) using a Shimadzu UV-1800 UV Spectrophotometer. Aqueous samples were prepared by taking 20 μL of aqueous 11.5 mM CA and adding either 4 μL water or 4 μL of 300 mM NaCl to achieve a final concentration of 9.57 mM CA and either no salt or 50 mM NaCl. Monomeric samples in 3:1 DMSO/H₂O were prepared by mixing 20 μL of aqueous 11.5 mM CA with 60 μL DMSO.

Absorbance spectroscopy on CA gels (1-5 μL , 9.57 mM CA, 0.83 wt% PDDA) that were placed in aqueous solutions containing 0.85 M pH 4 ascorbic acid and 19.5 μM catalyst for 18 hours were recorded on a NanoDrop ND-1000 UV/Vis Spectrophotometer (see Figure S12).

Fluorescence Spectroscopy

Fluorescence spectroscopy was performed using an ISS PC1 Spectrofluorometer in an L-configuration. Samples were prepared by injecting 10 μL of aqueous CA solution (115 μM , prepared by mixing 2 μL 11.5 mM CA with 98 μL water) into 0.99 mL of DMSO, water, or aqueous 50 mM NaCl. Emission spectra of CA solutions (1.15 μM , 1 mL) were measured in 10 mm quartz cuvettes, excited at 500 nm, and fluorescence intensity recorded between 515 and 765nm.

H₂ Evolution experiments

CA solutions were prepared by suspending the protonated CA in water, adding one equivalent (per mole) of an aqueous 4 M NaOH solution, and dissolved with the assistance of vortexing and bath sonication. Gels with PDDA were produced by addition of 20 μL of 5 wt% PDDA to 100 μL of aqueous CA solution (11.5 mM) to give a final CA concentration of 9.57 mM. CA-PDDA gels were prepared in a VWR Microwave Vial 7.7 mL (Catalog Number 89079-406), sealed with a rubber septum, and aged overnight (roughly 16 hours). Ascorbic acid solutions (1.7 M) were adjusted to pH 4 using 4 M NaOH (measured using a Fisher Scientific Accumet Research AR50 Dual Channel pH/Ion/Conductivity Meter, calibrated with pH 4.0 and

pH 7.0 standard solutions prior to pH adjustment). Ascorbic acid (690 $\mu\text{L}/\text{sample}$, $\sim 0.85\text{ M}$ ascorbic acid) and catalyst solutions (41.8 $\mu\text{L}/\text{sample}$, 400 μM) were mixed before addition of 700 μL to each tube of CA gel. Vials were sealed with a septum, further tightened with zip-ties, and wrapped in Parafilm to ensure proper sealing. After purging for 10 minutes with Argon, (chosen as we observed an increase in H_2 turnovers, possibly due to improved O_2 displacement) the samples were illuminated for 18 hours with a Schott Ace 1 light source equipped with a broadband 21 V, 150 W EKE halogen bulb and fiber optic goosenecks. Samples were placed approximately 1.5 cm from the fiber optic light source (power output 250 W/cm^2). For H_2 identification and quantification, a 300 μL aliquot was taken from the sample vial (7.7 mL headspace) and injected onto a gas chromatograph (Shimadzu GC-2014) equipped with a 5 \AA molecular sieve column, Ar carrier gas, and a thermal conductivity detector. Eight-point calibration curves for H_2 and N_2 were created using a standard (7% H_2 balanced with N_2) and integrated peak areas were used to determine the H_2 concentration in the sample headspace at STP.

Synthesis

General Synthesis: In a round-bottom flask equipped with a stir bar, one equivalent of perylene monoanhydride, one equivalent zinc acetate dihydrate, three equivalents of imidazole, and five equivalents of the appropriate amino alkyl acid were dissolved in dry DMF, 1 milliliter per milligram perylene monoanhydride. The mixture was sonicated briefly to disperse the solids before heating at 120 $^\circ\text{C}$ for two days. During this time, the cloudy mixture turned clear red-orange. After two days, a red solid is precipitated by pouring the DMF solution into 0.02 M HCl, filtered, rinsed with water, and dried in air.

Esterification: The solid PMI is suspended in 1:1 DCM/MeOH, cooled to 0 $^\circ\text{C}$, and thionyl chloride (SOCl_2) added slowly. Upon SOCl_2 addition, the yellow-orange suspension changed to a deep red, with all of the remaining solid dissolving quickly. After stirring overnight at room temperature, the volatiles were removed via rotary evaporator. The residue is soluble in DCM and chromatographed to remove a high R_f orange band (not collected) and unreacted carboxylic acid PMI. Alternatively, suspension of the L1 in DCM, followed by the addition of oxalyl chloride and several drops of DMF resulted in the complete dissolution of the PMI. After removal of the DCM and excess oxalyl chloride by rotary evaporation the red solid is suspended in DCM (in which the solid soluble), n-propanol added, and the solution allowed to stir

overnight. Removal of volatiles once more by rotary evaporation afforded the n-propyl ester whose solubility in DCM allowed for chromatographic purification.

After passing PMI esters through a silica gel column (gradient DCM to 2:98 MeOH:DCM), the material is purified further using recycling gel permeation chromatography (rGPC). Using the rGPC, it is possible to separate out several low-concentration impurities that were unable to be removed via silica gel chromatography (see Figure S1) To cleave the ester, the solid is dissolved in 98% sulfuric acid to yield a deep blue solution and one-quarter to one-half volume equivalent of water is added very carefully. After the addition, the solution is swirled to mix, during which the solution heats up drastically, and the resulting solution appears deep purple in color. The solution is allowed to sit overnight before precipitation in water, the precipitate filtered and washed thoroughly with water to remove any excess sulfuric acid. Alternatively, after precipitation, the suspension is centrifuged in a 15 mL tube, clear supernatant decanted, and precipitate vortexed with 15 mL of water. This process was repeated until the supernatant pH matched that of the water (pH 4-5). Samples were then flash-frozen and freeze-dried to remove any residual water.

The protonated CAs are poorly soluble in dichloromethane (DCM), acetonitrile, chloroform, acetone, and methanol (MeOH), mildly soluble in DMF and dimethylsulfoxide (DMSO), and most soluble in a 1:1 DCM/MeOH mixture.

Interestingly, when we attempted basic hydrolysis with lithium hydroxide, sodium hydroxide, or potassium hydroxide in THF/water mixtures, we observed minimal ester cleavage and under higher base concentrations partial imide hydrolysis instead.

L1

^1H NMR (499 MHz, DMSO- d_6) δ 8.73 (dd, $J = 7.7, 4.8$ Hz, 4H), 8.50 (d, $J = 8.5$ Hz, 2H), 8.17 – 8.00 (m, 2H), 7.74 (t, $J = 7.8$ Hz, 2H), 4.75 (s, 2H).

^{13}C NMR could not be obtained due to extremely poor solubility.

HR MS (M+Na): 402.07368 (Calc) 402.07314 (Found) Difference = 0.54 mDa

L2

^1H NMR (499 MHz, DMSO- d_6) δ 8.60 (dd, $J = 7.9, 6.3$ Hz, 4H), 8.39 (d, $J = 8.0$ Hz, 2H), 8.04 (d, $J = 8.1$ Hz, 2H), 7.69 (t, $J = 7.7$ Hz, 2H), 4.27 (dd, $J = 9.8, 5.8$ Hz, 2H), 2.70 – 2.55 (m, 2H).

^{13}C NMR (126 MHz, DMSO) δ 172.48, 162.84, 136.58, 133.77, 131.09, 131.01, 129.02, 128.33, 127.30, 126.96, 125.97, 124.52, 120.83, 120.24, 79.22, 79.16, 78.96, 78.69, 40.11, 40.02, 39.95, 39.85, 39.78, 39.69, 39.61, 39.52, 39.45, 39.35, 39.19, 39.02, 35.70, 32.19.

HR MS (M+Na): 416.08933 (Calc) 416.08894 (Found) Difference = 0.40 mDa

L3

^1H NMR (499 MHz, DMSO- d_6) δ 8.70 – 8.65 (m, 4H), 8.45 (d, J = 8.0 Hz, 2H), 8.06 (d, J = 8.1 Hz, 2H), 7.72 (t, J = 7.8 Hz, 2H), 4.11 (t, J = 7.0 Hz, 2H), 2.32 (t, J = 7.3 Hz, 2H), 1.91 (p, J = 7.1 Hz, 2H).

^{13}C NMR (101 MHz, dmsO) δ 173.98, 162.96, 136.23, 133.62, 130.86, 130.74, 128.80, 128.19, 127.12, 126.77, 125.71, 124.26, 120.62, 120.11, 39.99, 31.40, 23.04.

HR MS (M+Na): 430.10766 (Calc) 430.10711 (Found) Difference = 0.57 mDa

L4

^1H NMR (499 MHz, Chloroform- d) δ 8.41 (d, J = 8.0 Hz, 2H), 8.27 (dd, J = 7.7, 1.0 Hz, 2H), 8.20 (d, J = 8.1 Hz, 2H), 7.83 (d, J = 8.0 Hz, 2H), 7.55 (dd, J = 8.1, 7.4 Hz, 2H), 4.19 (t, J = 6.9 Hz, 2H), 2.43 (dd, J = 8.1, 5.9 Hz, 2H), 1.92 – 1.73 (m, 2H), 0.97 – 0.74 (m, 2H).

^{13}C NMR could not be obtained due to extremely poor solubility.

HR MS (M+Na): 444.12063 (Calc) 444.12076 (Found) Difference = -0.13 mDa

L5 synthesized previously

L7

^1H NMR (400 MHz, DMSO- d_6) δ 8.60 (dd, J = 8.0, 4.2 Hz, 4H), 8.39 (d, J = 7.9 Hz, 2H), 8.03 (d, J = 8.1 Hz, 2H), 7.68 (t, J = 7.8 Hz, 2H), 4.12 – 3.93 (m, 2H), 2.20 (t, J = 7.4 Hz, 2H), 1.64 (d, J = 8.1 Hz, 2H), 1.57 – 1.43 (m, 2H), 1.43 – 1.21 (m, 6H).

^{13}C NMR (126 MHz, DMSO) δ 174.62, 162.75, 136.18, 133.58, 130.83, 130.67, 128.63, 128.13, 127.05, 126.71, 125.61, 124.22, 120.56, 119.95, 33.81, 28.57, 28.55, 27.48, 26.57, 24.57 (peak at 40.23, obscured by DMSO, identified by HMBC measurement)

HR MS (M+Na): 486.16758 (Calc) 486.16947 (Found) Difference = -1.86 mDa

L9

^1H NMR (499 MHz, DMSO- d_6) δ 8.51 (dd, J = 12.8, 7.5 Hz, 4H), 8.30 (d, J = 7.8 Hz, 2H), 7.97 (d, J = 8.0 Hz, 2H), 7.63 (t, J = 7.8 Hz, 2H), 3.99 (t, J = 7.6 Hz, 2H), 2.17 (t, J = 7.4 Hz, 2H), 1.63 (t, J = 7.0 Hz, 2H), 1.47 (t, J = 7.2 Hz, 2H), 1.30 (dd, J = 36.8, 5.2 Hz, 10H).

^{13}C NMR (126 MHz, DMSO- d_6) δ 174.50, 162.91, 136.46, 133.76, 131.01, 130.92, 128.94, 128.35, 127.27, 125.93, 124.48, 124.45, 120.82, 120.26, 33.67, 28.82, 28.72, 28.54, 27.46, 26.58, 24.50. (NB – HMBC suggests additional carbons near 28.54 peak).

HR MS (M+Na): 514.19888 (Calc) 514.19944 (Found) Difference = -0.57 mDa

Recycling GPC Traces for CA Purification

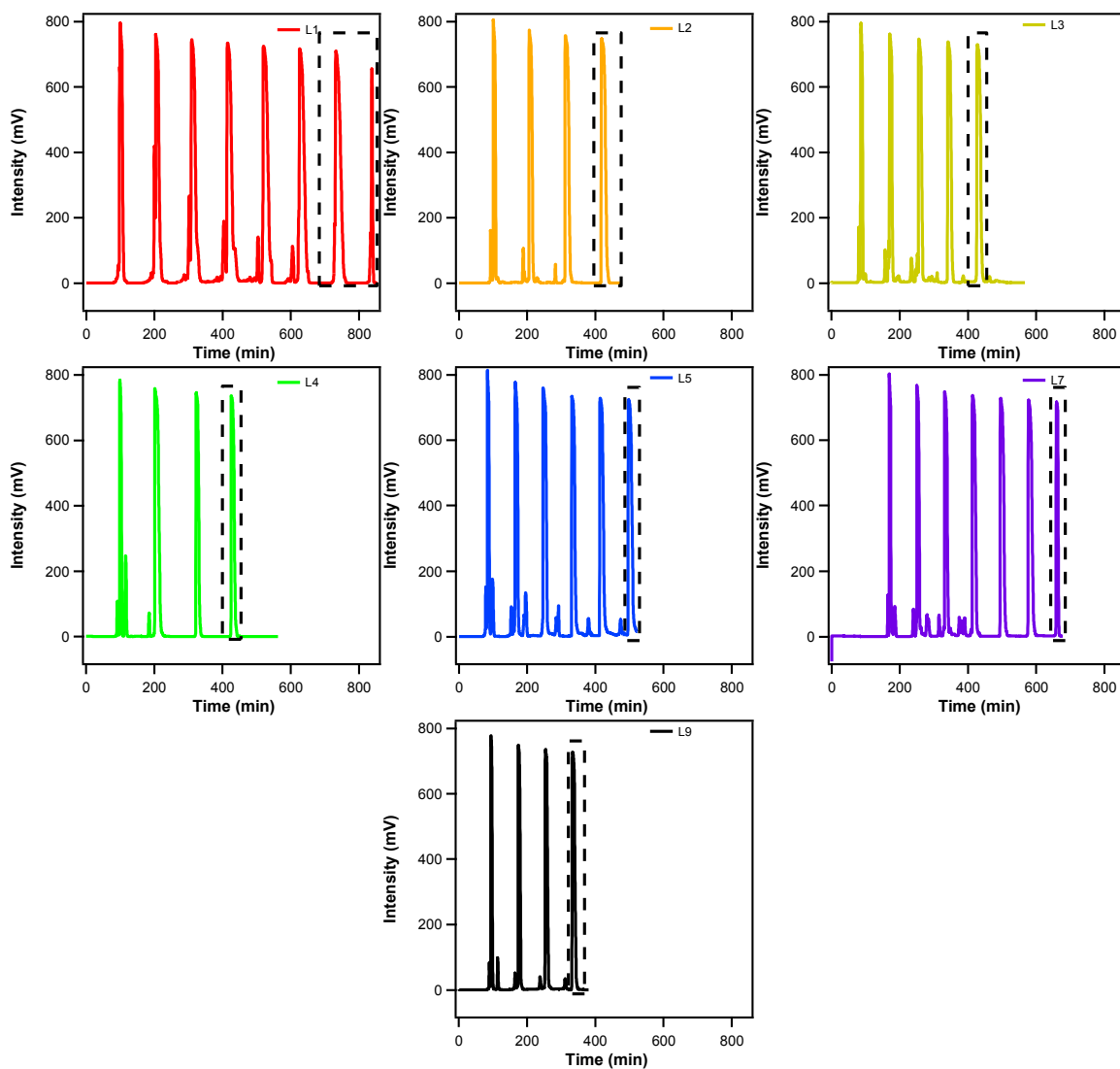


Figure S1: rGPC traces for the purification of CA linker series esters. The black, dotted box represents fractions collected from the GPC and used for experiments.

SAXS Pattern for CA Linker Series Without Added Salt

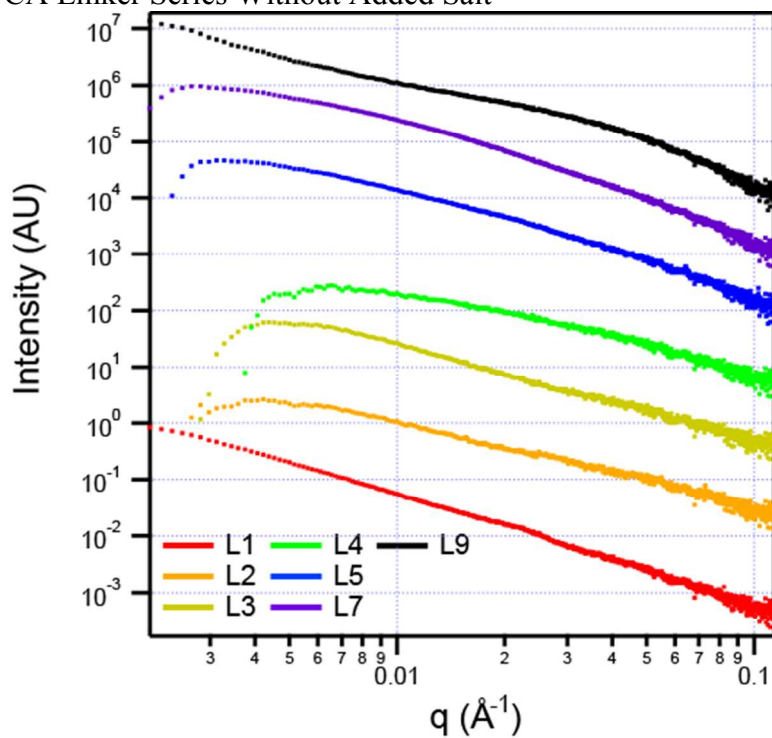
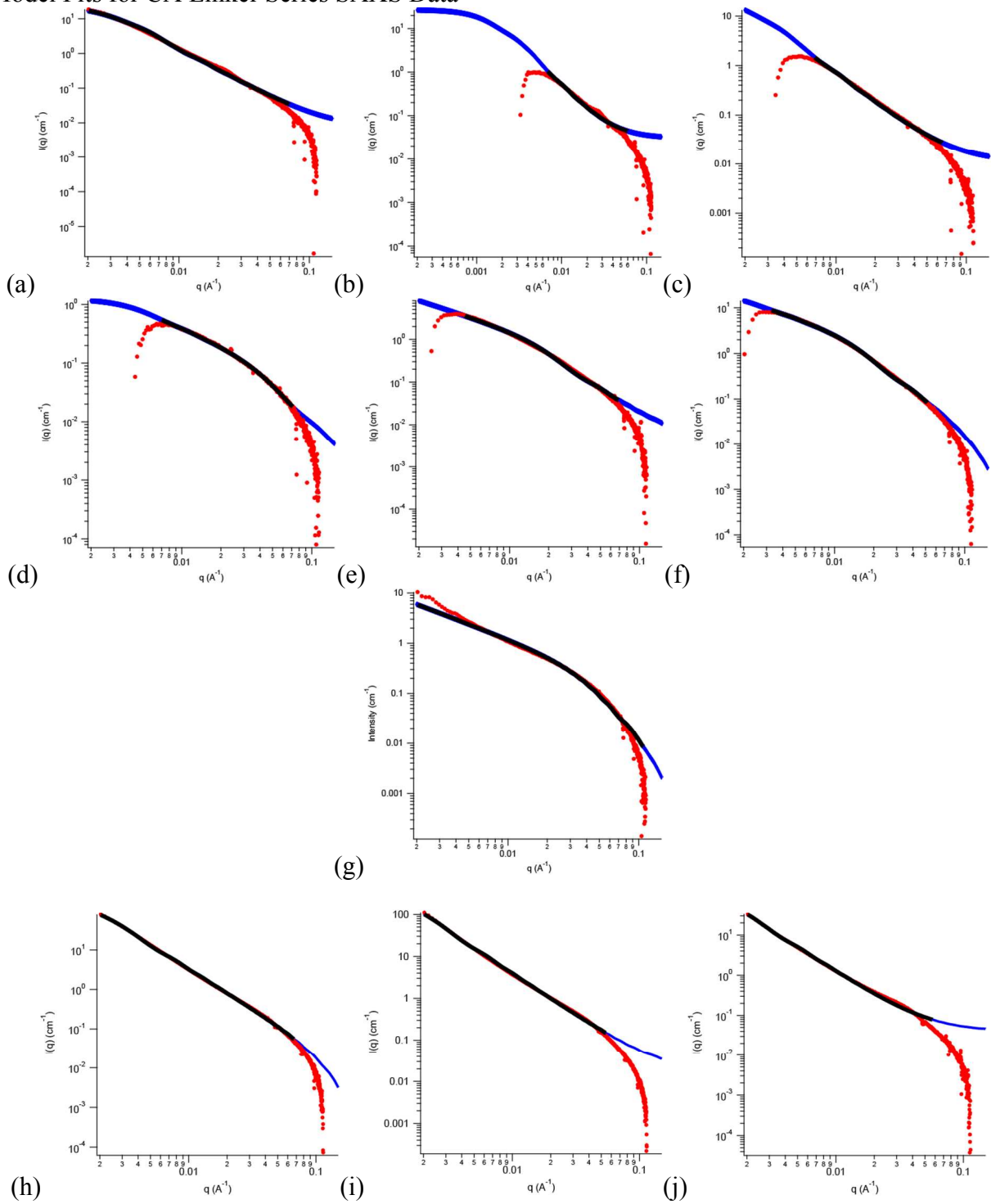


Figure S2. SAXS data for CA linker series' solution-state assemblies. All scattering data is recorded at 9.57 mM CA in water. As dissolved, **L2-L4** showed low scattering in the low q regime, suggesting structures less than 100 nm, consistent with the electron microscopy.

Model Fits for CA Linker Series SAXS Data



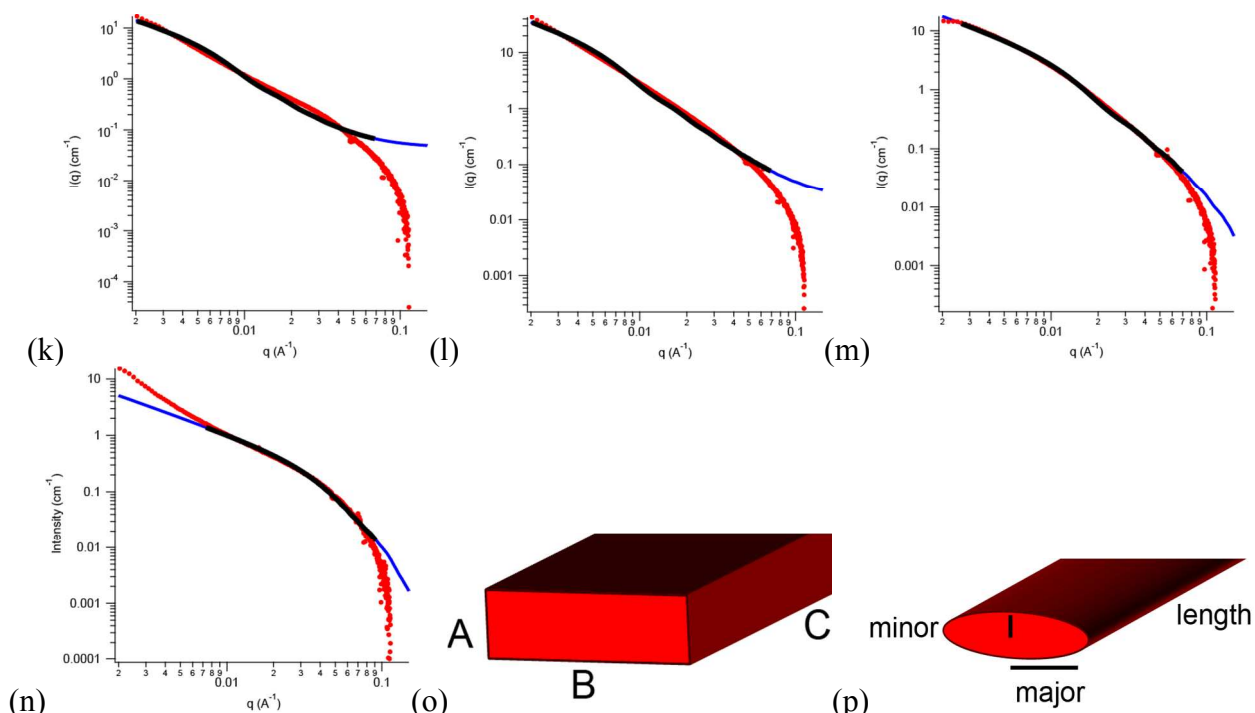


Figure S3. Fitting SAXS Data for CA Linker Series. The modelled data includes SAXS without (a-g) and in the presence of 50 mM NaCl (h-n). Molecules fit are L1 (a, h), L2 (b, i), L3 (c, j), L4 (d, k), L5 (e, l), L7 (f, m), and L9 (g, n). Molecules L1-L7 were fit using a Parallelepiped model (o), in which the nanostructures are approximated by rectangular blocks with thickness A, width B, and length C. Molecule L9 was fit best using an elliptical cylinder model (p), with a minor radius, major radius, and length as shown in the figure. For all model fits, the data is presented as red points, the model as blue points, and the fitted region as a black line.

Sample, no salt	Slope, 0.05-0.13	Width, B (Å)	Thickness, A (Å)	Sample, with salt	Slope, 0.05-0.13	Width (Å)	Thickness (Å)
L1	-1.8	660	12	L1	-2.1	1300	27
L2	-1.2	910	10	L2	-2.1	1600	9
L3	-1.1	930	10	L3	-2.1	1900	8
L4	-1	90	12	L4	-1.8	580	12
L5	-1.3	200	10	L5	-1.7	590	14
L7	-1	250	26	L7	-1.1	290	25
L9	-1.5	58	16	L9	-1.6	58	16

Table S1: Summary of SAXS slopes and model fitting for CA molecules without salt. Nanostructures are fit using the Parallelepiped form factor model, with the exception of L9, fit to an elliptical cylinder model. The longest dimension is omitted, as this value has a high degree of associated error. ^a length of major radius ^b length of minor radius

Solution state WAXS Data and Tables

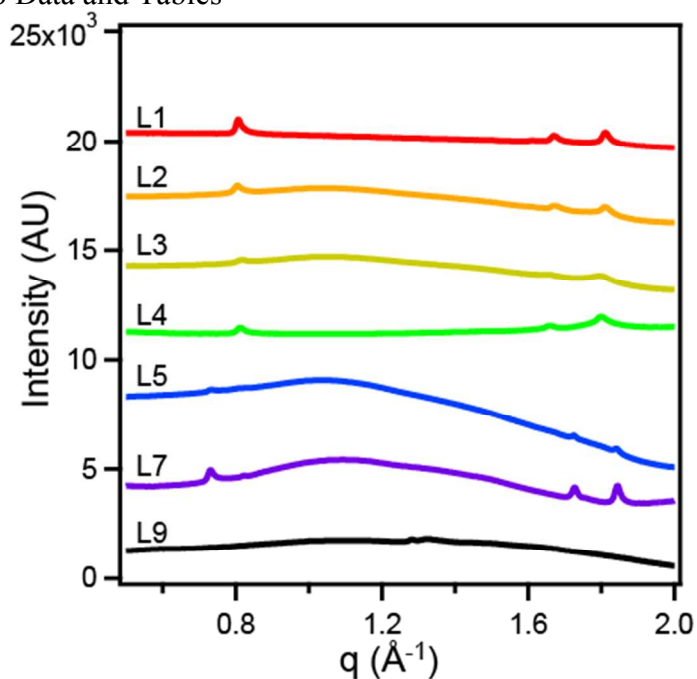


Figure S4: WAXS data of CA linker series in water (9.57 mM).

Table S2: WAXS diffraction peaks for CA linker series (each 9.57 mM) without added salt

Molecule	a^* (\AA^{-1})	b^* (\AA^{-1})	$(a+b)^*$ (\AA^{-1})
L1	0.807	1.68	1.81
L2	0.804	1.68	1.81
L3	0.817	1.66	1.80
L4	0.814	1.67	1.80
L5	0.735	1.73	1.84
L7	0.731	1.73	1.84
L9	-	-	-

Table S3: WAXS diffraction peaks for CA linker series (each 9.57 mM) in the presence of 50 mM PDDA

Molecule	a^* (\AA^{-1})	b^* (\AA^{-1})	$(a+b)^*$ (\AA^{-1})
L1	0.804	1.68	1.82
L2	0.804	1.67	1.81
L3	0.810	1.66	1.80
L4	0.816	1.65	1.80
L5	0.733	1.73	1.85
L7	0.731	1.73	1.84
L9	-	-	-

WAXS for CA Linker Series in NaCl

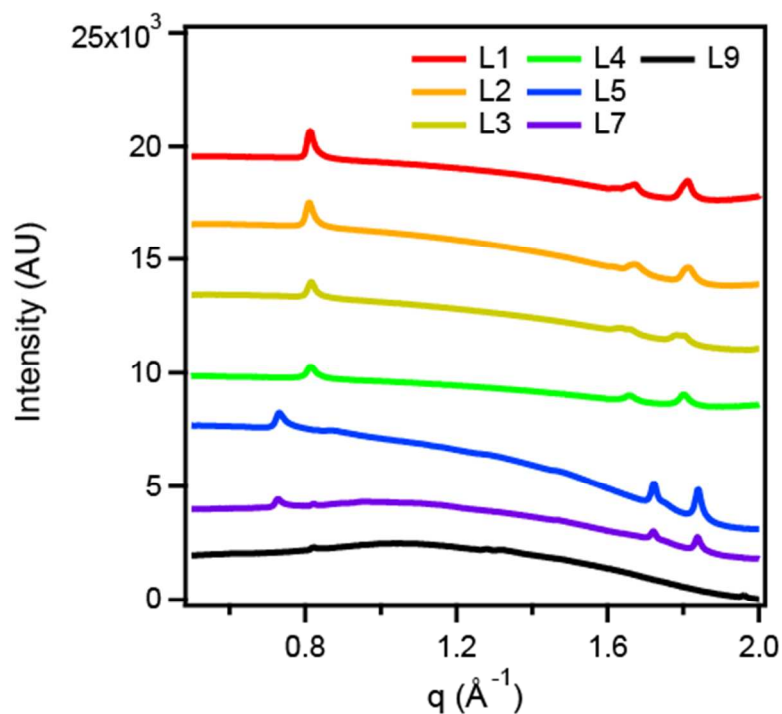


Figure S5. WAXS data on CA linker series solutions gelled with NaCl. All samples are prepared at 9.57 mM CA in aqueous 50 mM NaCl.

Table S4: Peak assignments for WAXS of CA linker series in aqueous 50 mM NaCl

Molecule	a^* (\AA^{-1})	b^* (\AA^{-1})	$(a+b)^*$ (\AA^{-1})	Edge-to-edge (\AA)	π stacking (\AA)	Angle ($^\circ$)	Area (\AA^2)
L1	0.814	1.67	1.81	7.73	3.76	86.3	29.0
L2	0.811	1.67	1.81	7.76	3.76	86.5	29.2
L3	0.816	1.63	1.78	7.72	3.85	86.6	29.7
L4	0.814	1.66	1.80	7.73	3.79	86.4	29.3
L5	0.732	1.72	1.84	8.59	3.65	87.2	31.3
L7	0.729	1.72	1.84	8.63	3.65	87.3	31.5
L9	-	-	-	-	-	-	-

Nanostructure Thickness versus Methylene Number

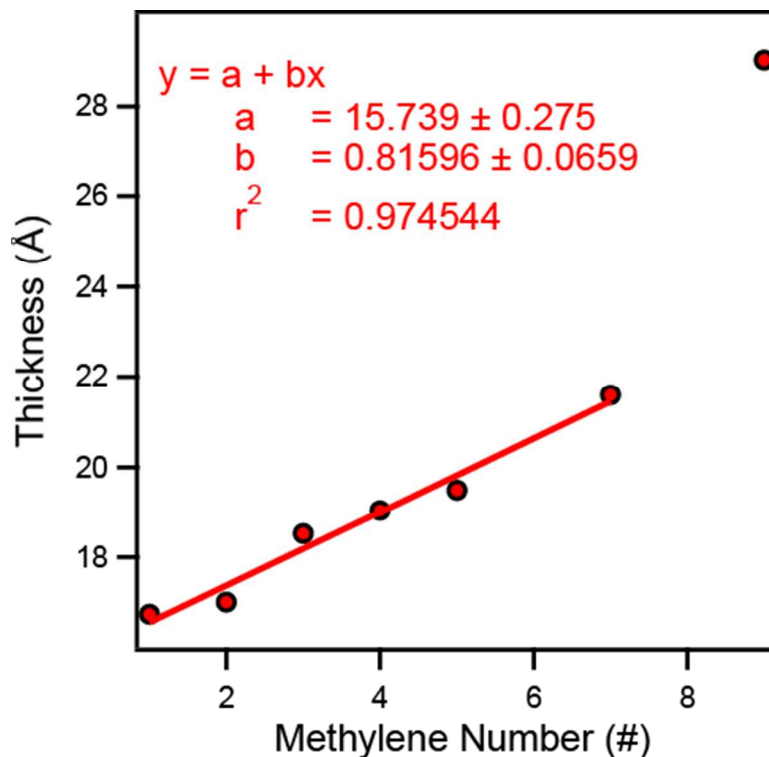


Figure S6: Plot of estimated nanostructure thickness from GIXS versus methylene number. The nanostructure thickness is estimated by calculating the real-space distance that corresponds to the primary scattering peak observed in the GIXS experiment.

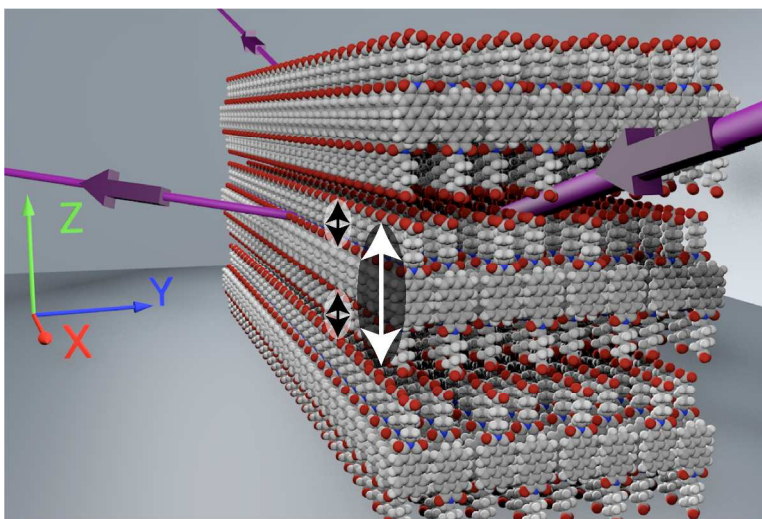


Figure S7: Diagram of proposed CA nanostructure packing on a substrate during GIXS experiment. The incident beam (purple arrow) is scattered in both the xy -plane and the z -axis. The white, double-headed arrow represents the nanostructure thickness while the black arrow represents the distance between PMI core and exterior surface carboxylates.

AFM Data on CA Linker Series

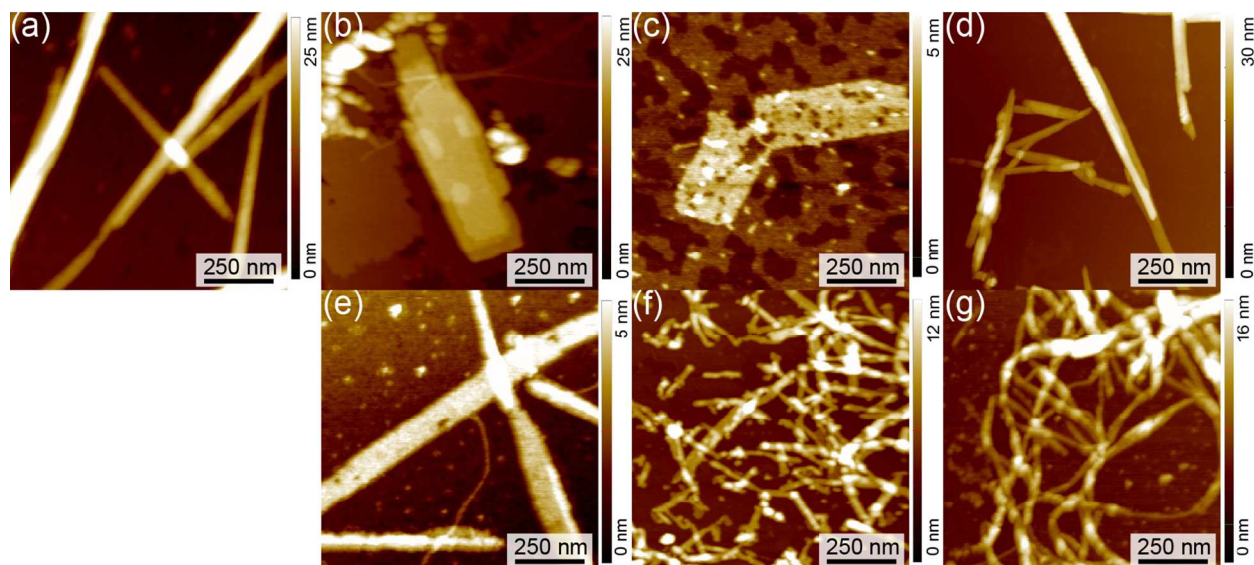


Figure S8: AFM images of (a) L1, (b) L2, (c) L3, (d) L4, (e) L5, (f) L7, (g) L9 on mica. Mica substrates were freshly cleaved, treated with aqueous 100 mM MgCl_2 , and washed with water before 4 μL of 115 μM CA solution was dropcast and allowed to dry.

GIXS Diffraction Peaks Tabulation

Table S5: 2D GIXS diffraction peak assignments for CA linker series films

Molecule	XY-Plane Peaks			Z-Axis Peaks	Off-axis Peaks	
	a^* (\AA^{-1})	b^* (\AA^{-1})	$(a+b)^*$ (\AA^{-1})	Scattering Peak (\AA^{-1})	q (\AA^{-1})	Spacing (\AA)
L1	0.835	1.73	1.88	0.376, 0.728, 1.10, 1.54	0.591	10.6
L2	0.844	1.72	1.86	0.370, 0.722	0.598	10.5
L3	0.835	1.72	1.87	0.339, 0.673	0.555	11.3
L4	0.850	1.74	1.88	0.330, 0.649	1.37	4.60
L5	0.772	1.79	1.92	0.322, 0.623	1.70	3.70
L7	0.764	1.79	1.91	0.291, 0.557		
L9	-	-	-	0.216, 0.397, 0.765		

Absorbance Data on CA Linker Series

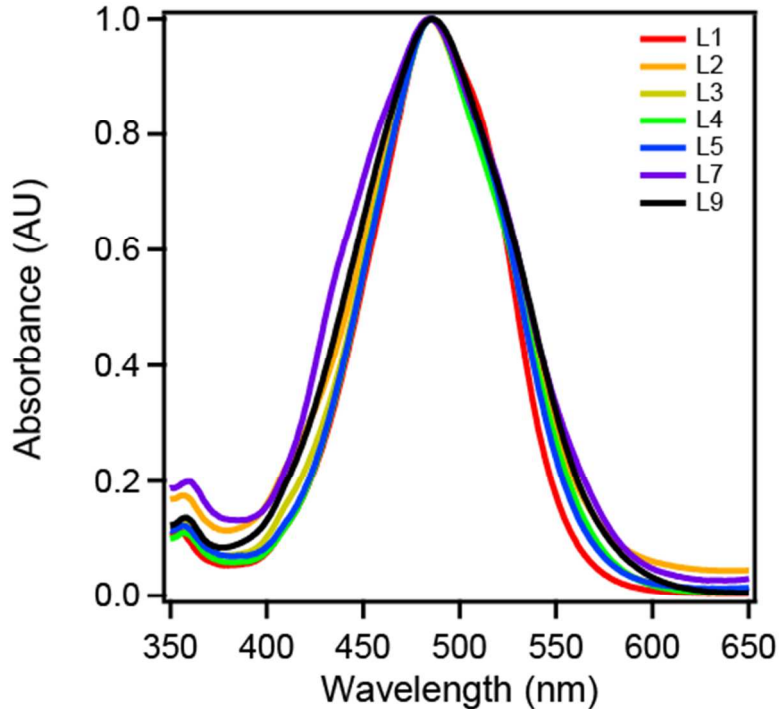


Figure S9: Absorbance data for CA linker series in 4:1 DMSO:water at 287.7 μM CA. Spectra were collected in a 0.05 mm quartz plate.

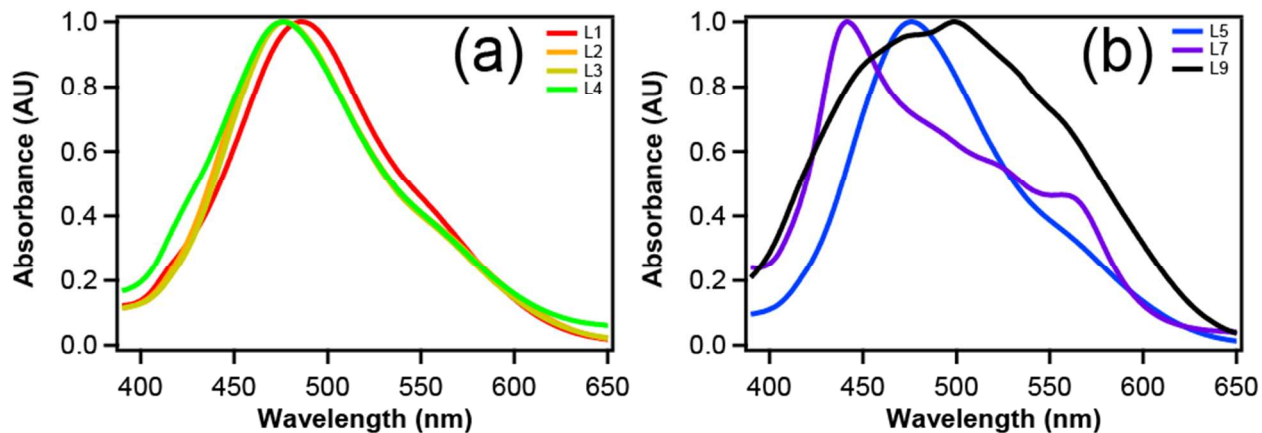


Figure S10: Absorbance data for CA linker series in water, no added salt, at 9.57 mM. Spectra were collected in a 0.05 mm quartz plate

Chemical Structure of **P2N2** Nickel Catalyst

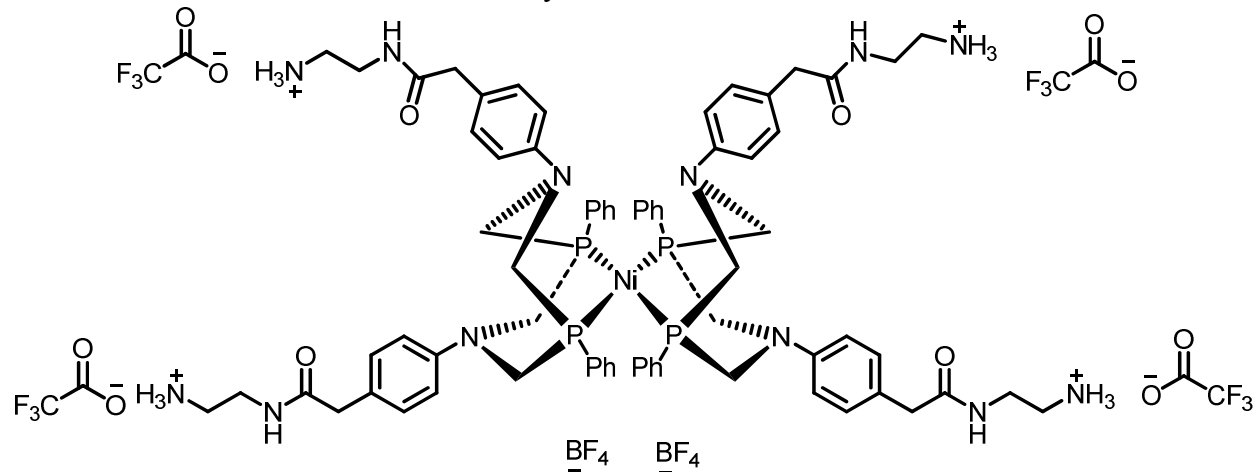


Figure S11: Chemical structure of **P2N2** nickel proton-reduction catalyst.

Absorbance of CA Gels in Photocatalysis Media

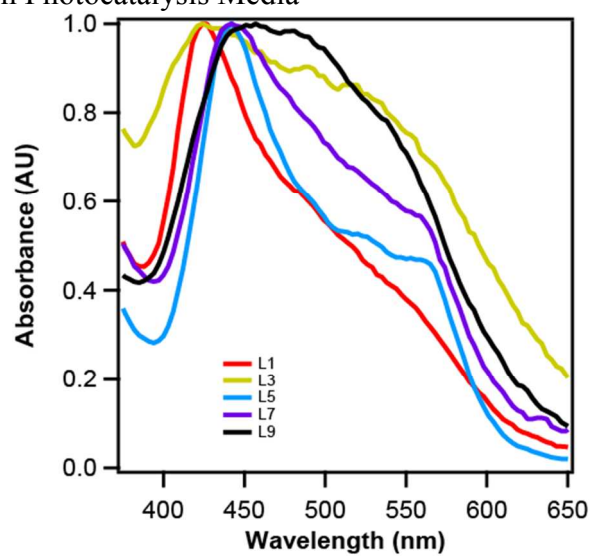


Figure S12: Normalized absorbance spectra of CA gels placed in aqueous solutions containing 0.85 M ascorbic acid and 19.5 μM catalyst.

SEM Images of CA-PDDA Gels

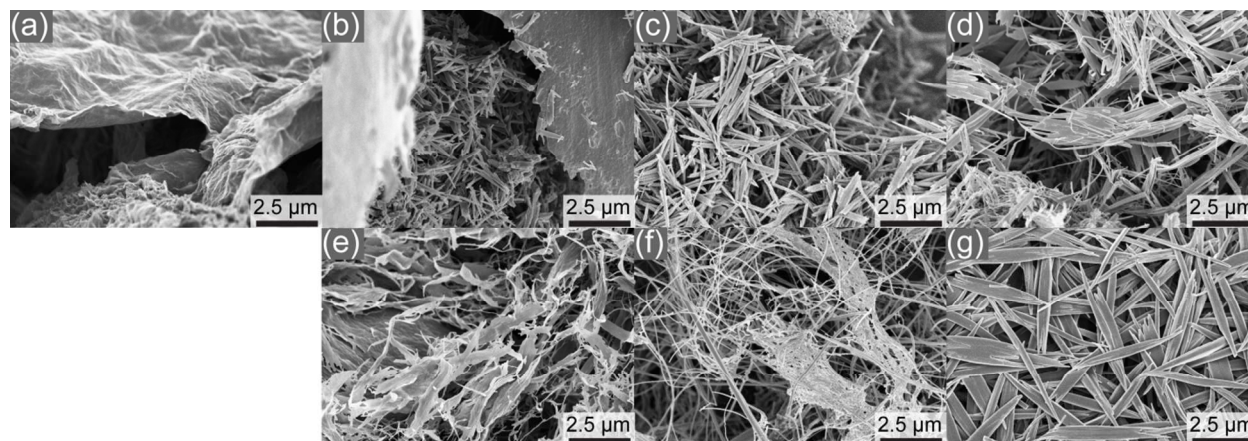


Figure S13: SEM images of PDDA gels of L1 (a), L2 (b), L3 (c), L4 (d), L5 (e), L7 (f), and L9 (g). Gels contain a final PMI concentration of 9.57 mM. Sample Preparation: Gels are placed in increasing ratios of ethanol to water, from 0% to 25%, 50%, 60%, 70%, 80%, 90%, 95%, and 100% ethanol. Ethanol samples are critical-point-dried, affixed to carbon tape on an aluminum stub, and then coated with 20 nm Os prior to imaging.

Images of CA Linker Series PDDA Gels in Aqueous Ascorbate Solutions

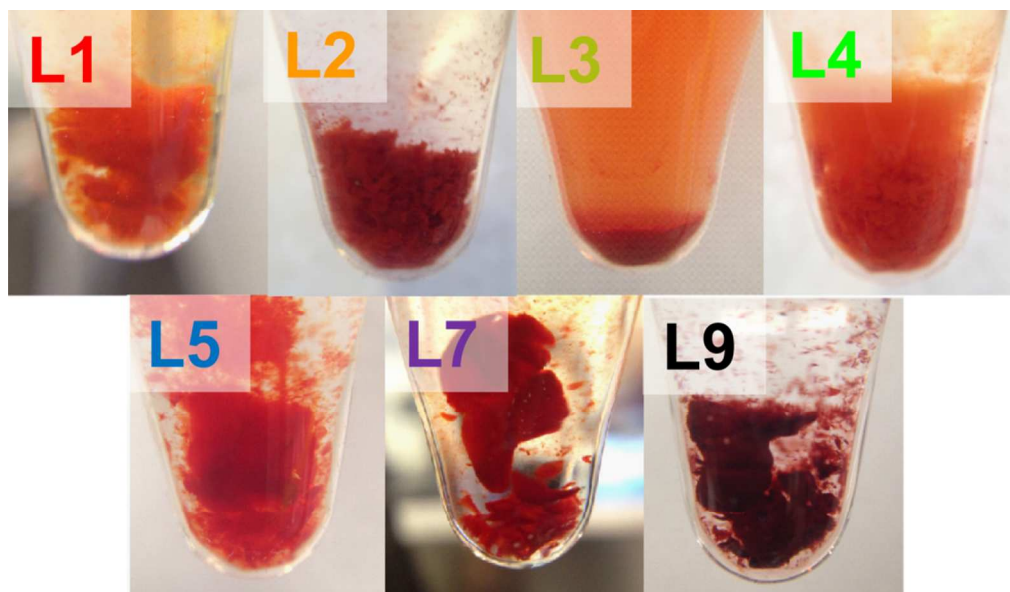


Figure S14: Images of CA-PDDA gels suspended in pH 4 ascorbate solutions (photographed in 7.7 mL microwave tubes).

H₂ Photosensitization Data from L3

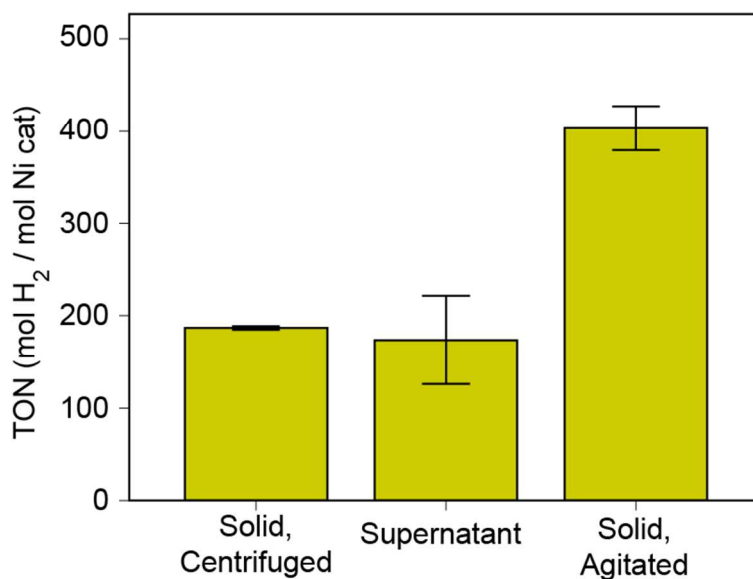


Figure S15: Photocatalytic H₂ evolution from L3. The mixture was centrifuged to localize the gel nanostructures at the bottom of the test tube and the supernatant removed. The localized gel and supernatant (left and center) were tested separately for photocatalysis. Localized gels were vortexed (right) and tested for photocatalysis as well.

Emission Data for CA Linker Series

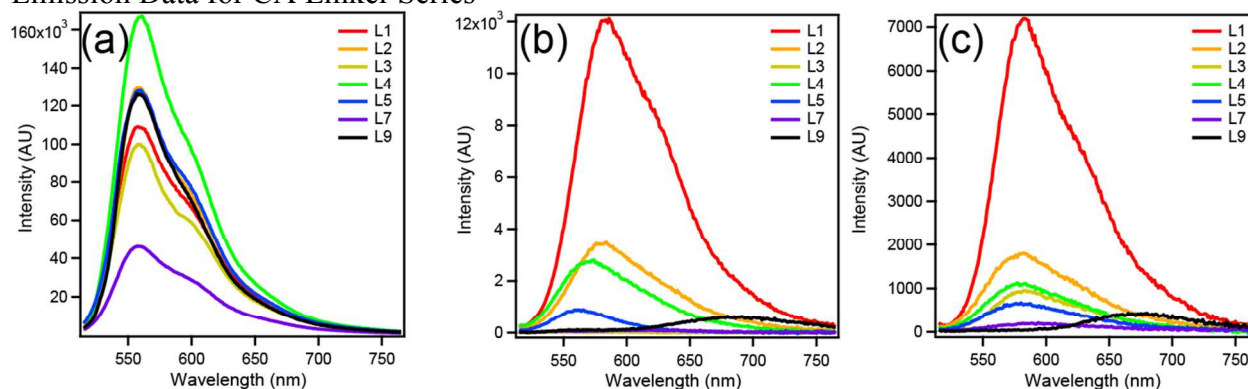


Figure S16: Emission data for CAs in (a) DMSO, (b) water, and (c) aqueous 50 mM NaCl. All samples are at roughly 1.15 μM CA. Samples are studied in 10 mm quartz cuvettes and excited at 500 nm.

Table S6. Summary of emission measurement data. Fluorescence maxima (λ_{max}) are determined from above data. Quenching percentage is determined by division of fluorescence maximum in aqueous 50 mM NaCl by the fluorescence maximum in DMSO and multiplying by 100%.

	DMSO		Water		Aqueous 50 mM NaCl		Quenching % (DMSO vs 50 mM NaCl)
	λ_{max}	Intensity	λ_{max}	Intensity	λ_{max}	Intensity	
L1	558	109000	586	12100	582	7199.2	93.4
L2	559	130000	584	3480	582	1800.8	98.6
L3	558	100000	-	-	584	960.6	99.0
L4	561	167000	574	2800	577	1131	99.3
L5	560	128000	563	900	580	678.5	99.5
L7	557	46000	617	114	594	207.43	99.6
L9	557	126000	691	654	680	446.29	99.6

References

- (1) Feiler, L.; Langhals, H.; Polborn, K. *Liebigs Ann.* **1995**, 1229.
- (2) Weingarten, A. S.; Kazantsev, R. V.; Palmer, L. C.; McClendon, M.; Koltonow, A. R.; Samuel, A. P. S.; Kiebal, D. J.; Wasielewski, M. R.; Stupp, S. I. *Nat. Chem.* **2014**, *6*, 964.